

SyntheticFur dataset for neural rendering

Le, Trung Poplin, Ryan Bertsch, Fred
 trungtle@google.com rpoplin@google.com fredbertsch@google.com
 Toor, Andeep Singh Oh, Margaret L.
 andeeptoor@google.com maggieoh@google.com

May 14, 2021

1 Abstract

We introduce a new dataset called SyntheticFur built specifically for machine learning training. The dataset consists of ray traced synthetic fur renders with corresponding rasterized input buffers and simulation data files. We procedurally generated approximately 140,000 images and 15 simulations with Houdini. The images consist of fur groomed with different skin primitives and move with various motions in a predefined set of lighting environments. We also demonstrated how the dataset could be used with neural rendering to significantly improve fur graphics using inexpensive input buffers by training a conditional generative adversarial network with perceptual loss. We hope the availability of such high fidelity fur renders will encourage new advances with neural rendering for a variety of applications.

2 Introduction

Fur is an important element of character design in films and video games to connect the viewers to these characters with empathetic emotions. Physically based rendering of hair and fur [16] [13] [27] model the hair fibers as dielectric cylinders to solve for the light rendering equation with ray tracing. Production ray tracing engines in films and animations can render fur with physically accurate visual quality and simulation [3]. However, real-time applications such as video games often cannot afford

the same budget due to the complexity of rendering dense hair strands with transparent material, and the expensive computational cost of physics simulation. Most commonly, the solution is to pre-render the strands into hair cards and significantly reduce the number of strands to simulate. Recent advancement in game engines introduce the new strand-based approach [23] [5] [20] for real-time interactive hair that improve over hair cards. However, implementation of real-time strand-based fur rendering is still a complex task.

The state of neural rendering [22] [18] has risen in popularity due to the increasing number of publicly available image datasets [4] [8] [9] [28] [24] for machine learning. Many of these techniques take advantage of deep learning’s effectiveness in solving image to image translation tasks. We recognize that we can bring the rendering quality of real-time fur closer to that of offline ray tracing with a similar approach and created the SyntheticFur dataset. We create the dataset specifically for deep learning from the ground up and so are able to make certain design decisions to help simplify training tasks including consistent image resolutions, backgrounds, lighting environments and conditions, fur materials, skin primitives, and simple motions. A synthetic dataset tailored for a particular training task has the advantage of being cleaner to process and simpler to analyze, with less feature engineering typically involved when working with a more generic photographic dataset.

To create the dataset, we use the Houdini soft-

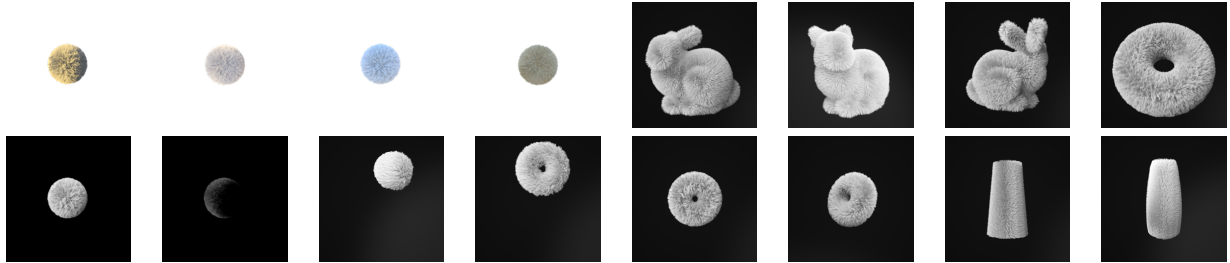


Figure 1: Examples of ground truth images in SyntheticFur.

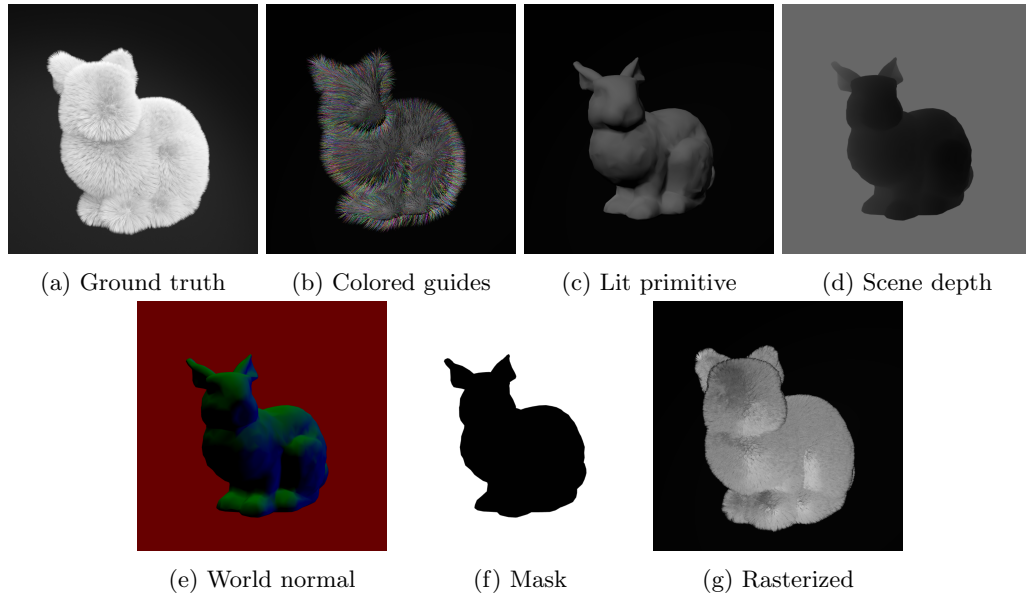


Figure 2: Each frame in the dataset contains a corresponding set of ground truth and input buffer images for training and evaluation.

ware to procedurally groom skin primitives with hair strands, and render the ground truth images with ray tracing using Mantra as the rendering engine. To generate the input images, we use the Houdini viewport rasterization of the same view to closely represent common image buffers generated by a game engine. We construct several scenes of a variety of different skin primitives and motions under predefined lighting conditions.

For modeling, we use a conditional generative adversarial network (cGAN). The model takes as inputs a set of rasterized image buffers and computes GAN loss and perceptual loss against the ray traced ground truth image. We do not use the simulation data here but note that it might be a fruitful direction for future work.

In summary, our contributions are:

- A high quality synthetic fur dataset with images and simulation data.
- An image-to-image model that uses this dataset to transform from inexpensive inputs to high quality renders.

3 Related Work

There are many image datasets freely available for use in computer vision and machine learning research, from more general images such as ImageNet [4] [8] [28], celebrity faces [15], or 3D human hair [24]. However, there are no datasets created for fur on more primitive geometries. Authoring and rendering fur with ray tracing to achieve photorealistic quality is a time consuming process; as such, our contribution can help save the time and expertise required to create such a dataset.

Neural rendering has many applications, ranging from denoising [11], supersampling [26] [25], neural radiance field [18] [17], volumetric cloud rendering [14], to hair synthesis [1] [19] [21] and rendering [2].

4 Method

4.1 Architecture

To validate iterations of our dataset, we use a GAN [6] image to image model. Our network consists of a convolutional UNet generator \mathcal{G} with skip connections and a convolutional discriminator \mathcal{D} (see fig. 3). Instance normalization is applied to the convolutional layers in \mathcal{G} and \mathcal{D} . We use Adam for optimization. We use WGAN-GradientPenalty loss [7], perceptual loss [12] and L1 loss. Our model uses data augmentation with random horizontal flipping and vertical flipping to increase the training sample diversity.

4.2 Conditioning inputs

We use rasterized buffers as conditioning inputs that propagate through \mathcal{G} and \mathcal{D} . The input images are generated as 512x512 patches to better fit into memory. The patches are sampled based on the Mask buffer to maximize using samples that contain the region of fur we want the model to observe.

5 Dataset Preparation

The dataset consists of several different parts. We provide the 3D groom assets that are used to render the fur, the rendered images of the fur, and a variety of representations that are cheap to calculate from a game engine. Finally, we include the full high quality simulations of fur positions.

Groom asset. We use the Houdini software to procedurally generate the groom asset. Starting with a base geometry, or the skin primitive, we distribute guide curves evenly along the skin primitive surface and added small amounts of curliness and lifting so that the fur would stick out.

Ground truth images. To render the ground truth images, we used Houdini’s rendering engine Mantra to ray trace the groom asset, producing the high quality ground truth images. Due to the complexity of ray tracing fur, which has a high density of polygons and transparent materials, the process of rendering each frame can take up several minutes, or hours for a full video sequence on a local machine. We opted

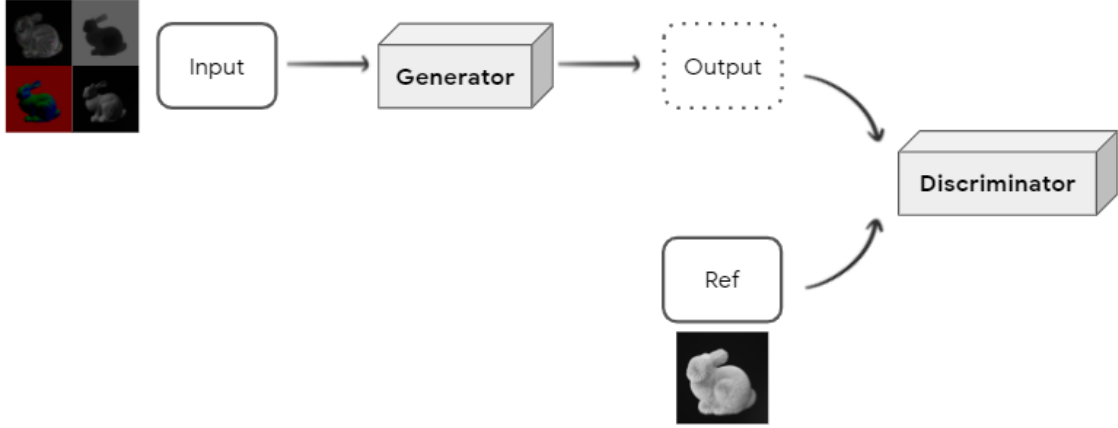


Figure 3: Architecture of the conditional GAN. The inputs are rasterized input buffers, and the ground truth reference is the ray traced image.

to use Google Zync Cloud Rendering infrastructure to speed up the process. This has the advantage of distributing the rendering jobs across multiple machines, significantly reducing the time that it would normally take for fur rendering.

Input buffers images. To create the various input buffer images, we use the viewport of Houdini to render the scene depth, world normal, lit primitive, mask and guide curves buffers. Because the Houdini viewport is a real-time rasterized rendering engine, our input buffers would be equivalent to captures taken from other similar real-time rendering engines. We use the mask buffer only during this step to select relevant path samples that are more likely to contain fur over uninteresting details like the dark backgrounds.

Simulation Data. We use the Alembic format, as it has a widely supported API, to export the simulation data for each scene sequence. We added a custom attribute to specify the number of segments per strand.

Note: To provide more diversity in lighting, we rotate our light rig exactly twice for 360 frames each. Once along the camera’s up vector, and once along the camera’s forward vector. Therefore, it can be useful to compare results from frame 1, 180, 360, 540).

6 Results

Note: All images are generated at resolution 1024 x 1024, but are cropped and resized here to be conveniently displayed. Please see the supplemental materials for the full resolution images.

We train using a combination of different input buffer types. We find that supplying the guide curves, lit primitive, and scene depth inputs provide the best qualitative visual results. The model is able to infer lighting directions from the diffuse shading of the skin primitives, without having to use additional lighting or shadow information.

We show our results with different lighting environment scenes (fig. 4, 5) and fur generated on unseen skin primitives (fig. 6, 7).

Using the SyntheticFur dataset, we were able to achieve significantly better visual quality fur rendering than a rasterizer. According to our informal survey of artists, it was significantly closer to offline ray tracing quality (fig. 8). In particular, we were able to create better soft shadows compared to strand-based real time renderers.

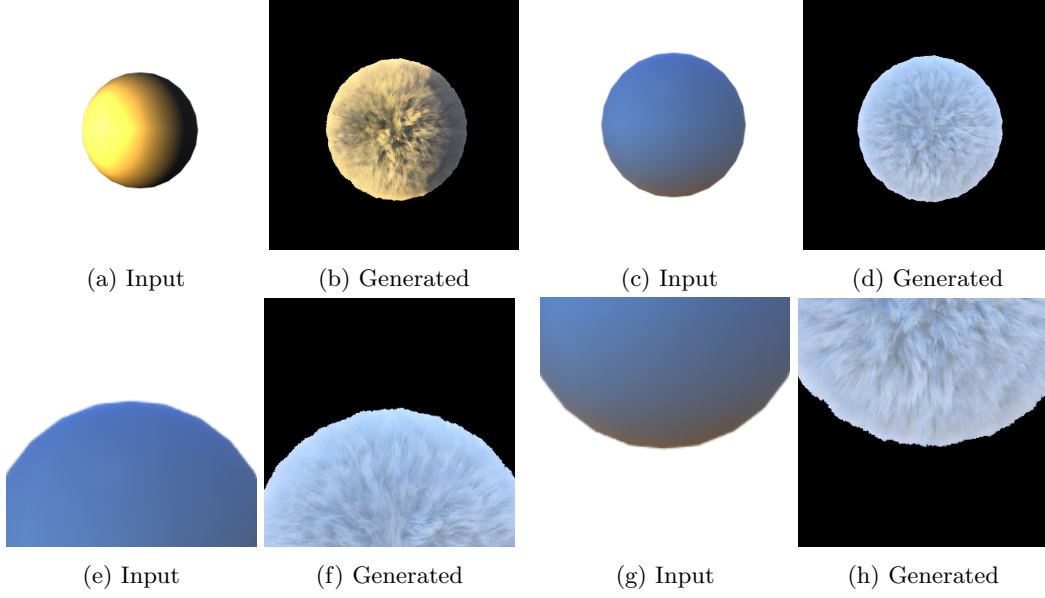


Figure 4: By providing different lit primitive shadings in addition to the guide curves, the model can generalize to a different lighting environment. In (e), (f), the lighting is bluer at the top of the sphere, compared to the yellowish color at the bottom of the sphere (g), (h)

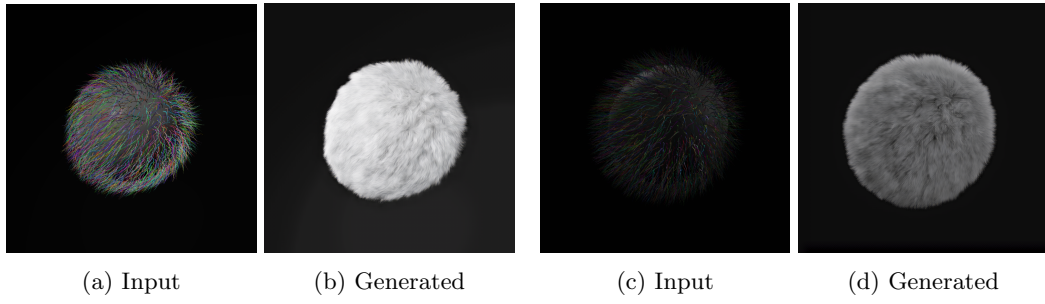


Figure 5: Fur is brighter or darker according to the light intensity.

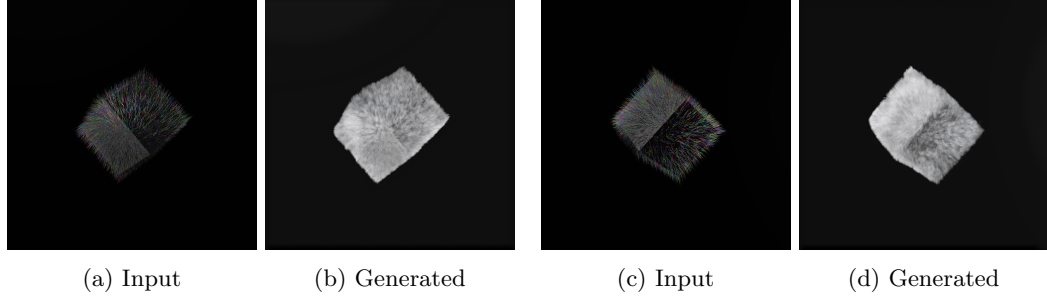


Figure 6: Fur correctly groomed on sharp edges, and shaded the two sides of the boxes correctly based on the diffuse input.

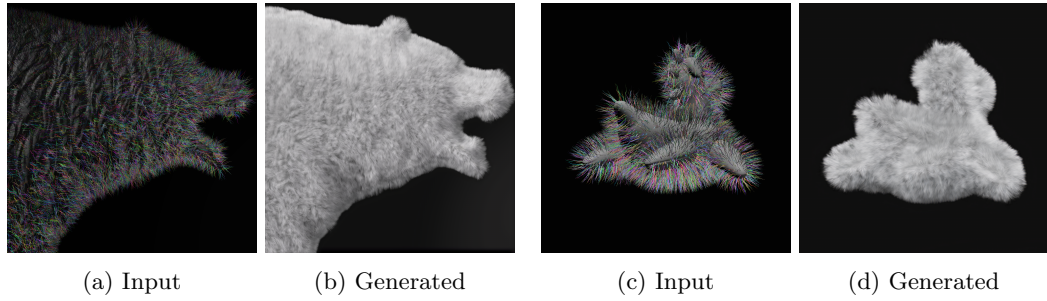
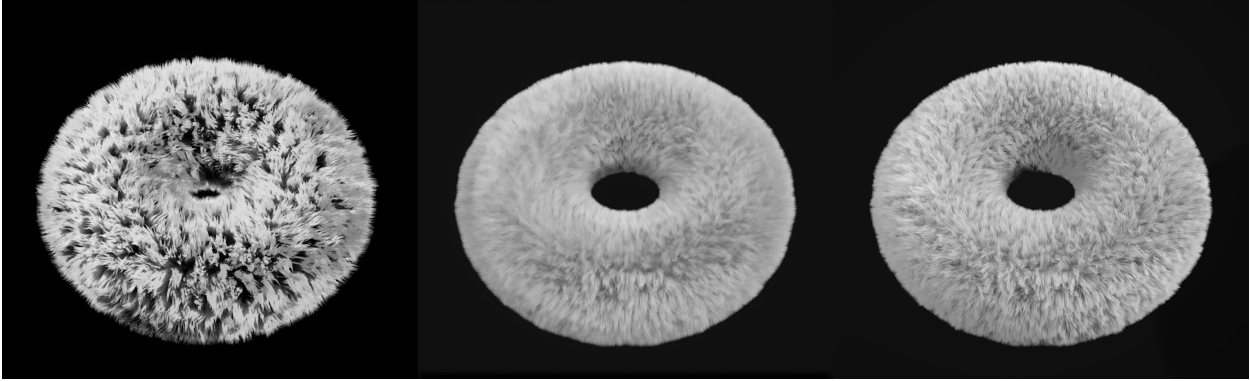


Figure 7: Generalization on more complex skin primitives.



(a) Bunny



(b) Torus

Figure 8: Comparison of generated images against real-time and offline engines. From left to right: (Real-time) Unreal 4.25, Ours, (Offline) Houdini 17.0.

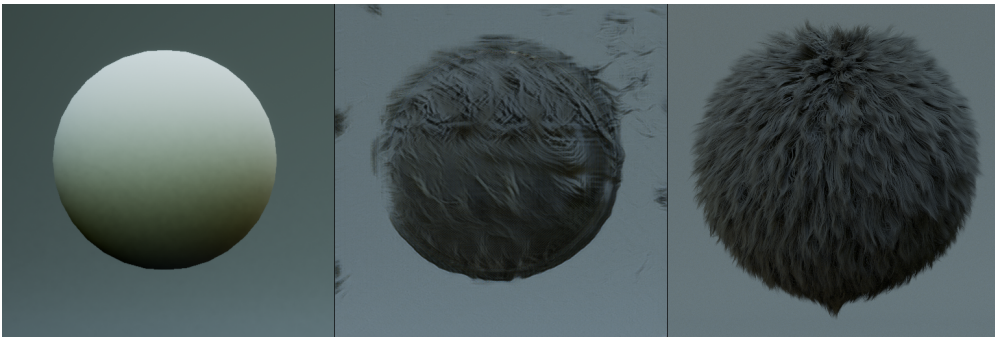


Figure 9: Without the additional guide curve inputs, it is challenging for the model to generate the fur strands properly.

7 Discussion

7.1 Rendering

We are in the early stage of prototyping the model, with the eventual goal to create an end-to-end pipeline from simulation inputs to rendering outputs for real-time applications. Under the right conditions, our model has shown that it is possible to achieve higher results compared to real-time strand-based approach.

However, to truly be beneficial for real-time applications, we need to improve on performance and add additional control knobs to enable programmers and artists to take advantage of this method. This could be accomplished by using dedicated compute shaders to run inference of a simpler pre-trained model. We would like to implement a modular solution that allows for easy integration into existing workflows of modern rendering engines.

Our approach also has the following additional limitations:

- Our generated outputs cannot yet learn proper alpha blending, and therefore will create artifacts during object occlusion.
- While the frames generated are generally stable, more work can be done to further improve temporal consistency.
- Our model is sensitive to gamma changes of input images if they have not been observed during training.
- At very sharp grazing angles, fur strands can become very blurry and lose definition.

7.2 Simulation

We are at the beginning of exploring a neural physics model that use the simulation data to predict fur motion. One approach is to use the hair segment end points to project onto a unit sphere relative to the camera view direction. The projection in this subspace can enable training a 2D CNN more effectively. The points can then be projected back into camera/view space to be used in conjunction with

the rendering network. A similar approach to neural physics is demonstrated for cloth [10].

8 Acknowledgement

We would like to thank Omar Skarsvåg and Aaron Parisi for their contributions in creating the dataset, tools to generate training results, and many helpful discussions, and Google Brain and Stadia for enabling this work.

References

- [1] M. Chai, T. Shao, H. Wu, Y. Weng, and K. Zhou. Autohair: Fully automatic hair modeling from a single image. *ACM Trans. Graph.*, 35(4), July 2016. ISSN 0730-0301. doi: 10.1145/2897824.2925961. URL <https://doi.org/10.1145/2897824.2925961>.
- [2] M. Chai, J. Ren, and S. Tulyakov. Neural hair rendering, 2020.
- [3] M. J.-Y. Chiang, B. Bitterli, C. Tappan, and B. Burley. A practical and controllable hair and fur model for production path tracing. In *ACM SIGGRAPH 2015 Talks*, SIGGRAPH '15, New York, NY, USA, 2015. Association for Computing Machinery. ISBN 9781450336369. doi: 10.1145/2775280.2792559. URL <https://doi.org/10.1145/2775280.2792559>.
- [4] J. Deng, W. Dong, R. Socher, L.-J. Li, K. Li, and L. Fei-Fei. Imagenet: A large-scale hierarchical image database. In *2009 IEEE conference on computer vision and pattern recognition*, pages 248–255. Ieee, 2009.
- [5] Frostbite Engine. Strand-based hair rendering in frostbite, 2019. URL http://advances.realtimerendering.com/s2019/hair-presentation_final.pdf.
- [6] I. J. Goodfellow, J. Pouget-Abadie, M. Mirza, B. Xu, D. Warde-Farley, S. Ozair, A. Courville, and Y. Bengio. Generative adversarial networks, 2014.

- [7] I. Gulrajani, F. Ahmed, M. Arjovsky, V. Dumoulin, and A. Courville. Improved training of wasserstein gans, 2017.
- [8] S. W. Hasinoff, D. Sharlet, R. Geiss, A. Adams, J. T. Barron, F. Kainz, J. Chen, and M. Levoy. Burst photography for high dynamic range and low-light imaging on mobile cameras. *ACM Transactions on Graphics (Proc. SIGGRAPH Asia)*, 35(6), 2016.
- [9] J. Hazelzet. Images of lego bricks, 2018. URL <https://www.kaggle.com/joosthazelzet/lego-brick-images>.
- [10] D. Holden, B. C. Duong, S. Datta, and D. Nowrouzezahrai. Subspace neural physics: Fast data-driven interactive simulation. In *Proceedings of the 18th Annual ACM SIGGRAPH/Eurographics Symposium on Computer Animation*, SCA '19, New York, NY, USA, 2019. Association for Computing Machinery. ISBN 9781450366779. doi: 10.1145/3309486.3340245. URL <https://doi.org/10.1145/3309486.3340245>.
- [11] V. Jain and S. Seung. Natural image denoising with convolutional networks. In D. Koller, D. Schuurmans, Y. Bengio, and L. Bottou, editors, *Advances in Neural Information Processing Systems*, volume 21. Curran Associates, Inc., 2009. URL <https://proceedings.neurips.cc/paper/2008/file/c16a5320fa475530d9583c34fd356ef5-Paper.pdf>.
- [12] J. Johnson, A. Alahi, and L. Fei-Fei. Perceptual losses for real-time style transfer and super-resolution, 2016.
- [13] J. T. Kajiya and T. L. Kay. Rendering fur with three dimensional textures. In *Proceedings of the 16th Annual Conference on Computer Graphics and Interactive Techniques*, SIGGRAPH '89, page 271–280, New York, NY, USA, 1989. Association for Computing Machinery. ISBN 0897913124. doi: 10.1145/74333.74361. URL <https://doi.org/10.1145/74333.74361>.
- [14] S. Kallweit, T. Müller, B. McWilliams, M. Gross, and J. Novák. Deep scattering. *ACM Transactions on Graphics*, 36(6):1–11, Nov 2017. ISSN 1557-7368. doi: 10.1145/3130800.3130880. URL <http://dx.doi.org/10.1145/3130800.3130880>.
- [15] Z. Liu, P. Luo, X. Wang, and X. Tang. Deep learning face attributes in the wild. In *Proceedings of International Conference on Computer Vision (ICCV)*, December 2015.
- [16] S. R. Marschner, H. W. Jensen, M. Cammarano, S. Worley, and P. Hanrahan. Light scattering from human hair fibers. In *ACM SIGGRAPH 2003 Papers*, SIGGRAPH '03, page 780–791, New York, NY, USA, 2003. Association for Computing Machinery. ISBN 1581137095. doi: 10.1145/1201775.882345. URL <https://doi.org/10.1145/1201775.882345>.
- [17] R. Martin-Brualla, N. Radwan, M. S. M. Sajjadi, J. T. Barron, A. Dosovitskiy, and D. Duckworth. NeRF in the Wild: Neural Radiance Fields for Unconstrained Photo Collections. In *CVPR*, 2021.
- [18] B. Mildenhall, P. P. Srinivasan, M. Tancik, J. T. Barron, R. Ramamoorthi, and R. Ng. Nerf: Representing scenes as neural radiance fields for view synthesis. In *ECCV*, 2020.
- [19] S. Saito, L. Hu, C. Ma, H. Ibayashi, L. Luo, and H. Li. 3d hair synthesis using volumetric variational autoencoders. *ACM Trans. Graph.*, 37(6), Dec. 2018. ISSN 0730-0301. doi: 10.1145/3272127.3275019. URL <https://doi.org/10.1145/3272127.3275019>.
- [20] R. Taillardier and J. Valdes. Every strand counts: Physics and rendering behind frostbite’s hair, Dec 2020. URL <https://youtu.be/ool2E8SQPGU>.
- [21] Z. Tan, M. Chai, D. Chen, J. Liao, Q. Chu, L. Yuan, S. Tulyakov, and N. Yu. Michigan: Multi-input-conditioned hair image generation for portrait editing. *ACM Trans. Graph.*, 39(4), July 2020. ISSN 0730-0301. doi: 10.

- 1145/3386569.3392488. URL <https://doi.org/10.1145/3386569.3392488>.
- [22] A. Tewari, O. Fried, J. Thies, V. Sitzmann, S. Lombardi, K. Sunkavalli, R. Martin-Brualla, T. Simon, J. Saragih, M. Nießner, R. Pandey, S. Fanello, G. Wetzstein, J.-Y. Zhu, C. Theobalt, M. Agrawala, E. Shechtman, D. B. Goldman, and M. Zollhöfer. State of the art on neural rendering, 2020.
 - [23] Unreal Engine. Hair rendering and simulation, 2020. URL <https://docs.unrealengine.com/en-US/WorkingWithContent/Hair/index.html>.
 - [24] USC. Usc-hairsalon: A 3d hairstyle database for hair modeling, 2015. URL <http://www-scf.usc.edu/~liwenhu/SHM/database.html>.
 - [25] A. Watson. Deep learning techniques for super-resolution in video games, 2020.
 - [26] L. Xiao, S. Nouri, M. Chapman, A. Fix, D. Lanman, and A. Kaplanyan. Neural supersampling for real-time rendering. *ACM Trans. Graph.*, 39(4), July 2020. ISSN 0730-0301. doi: 10.1145/3386569.3392376. URL <https://doi.org/10.1145/3386569.3392376>.
 - [27] L.-Q. Yan, H. W. Jensen, and R. Ramamoorthi. An efficient and practical near and far field fur reflectance model. *ACM Trans. Graph.*, 36(4), July 2017. ISSN 0730-0301. doi: 10.1145/3072959.3073600. URL <https://doi.org/10.1145/3072959.3073600>.
 - [28] F. Yu, A. Seff, Y. Zhang, S. Song, T. Funkhouser, and J. Xiao. Lsun: Construction of a large-scale image dataset using deep learning with humans in the loop, 2016.

9 Supplemental Materials

Ground truth (video): https://youtu.be/5uraQu_5Tyg.

Inference comparison, Bunny (video): https://youtu.be/_cKmDsjYLbE.

Inference comparison, Torus (video) : <https://youtu.be/rPo8k63OPWI>.

Dataset website link: <https://github.com/google-research-datasets/synthetic-fur>

9.1 Additional GAN-generated images

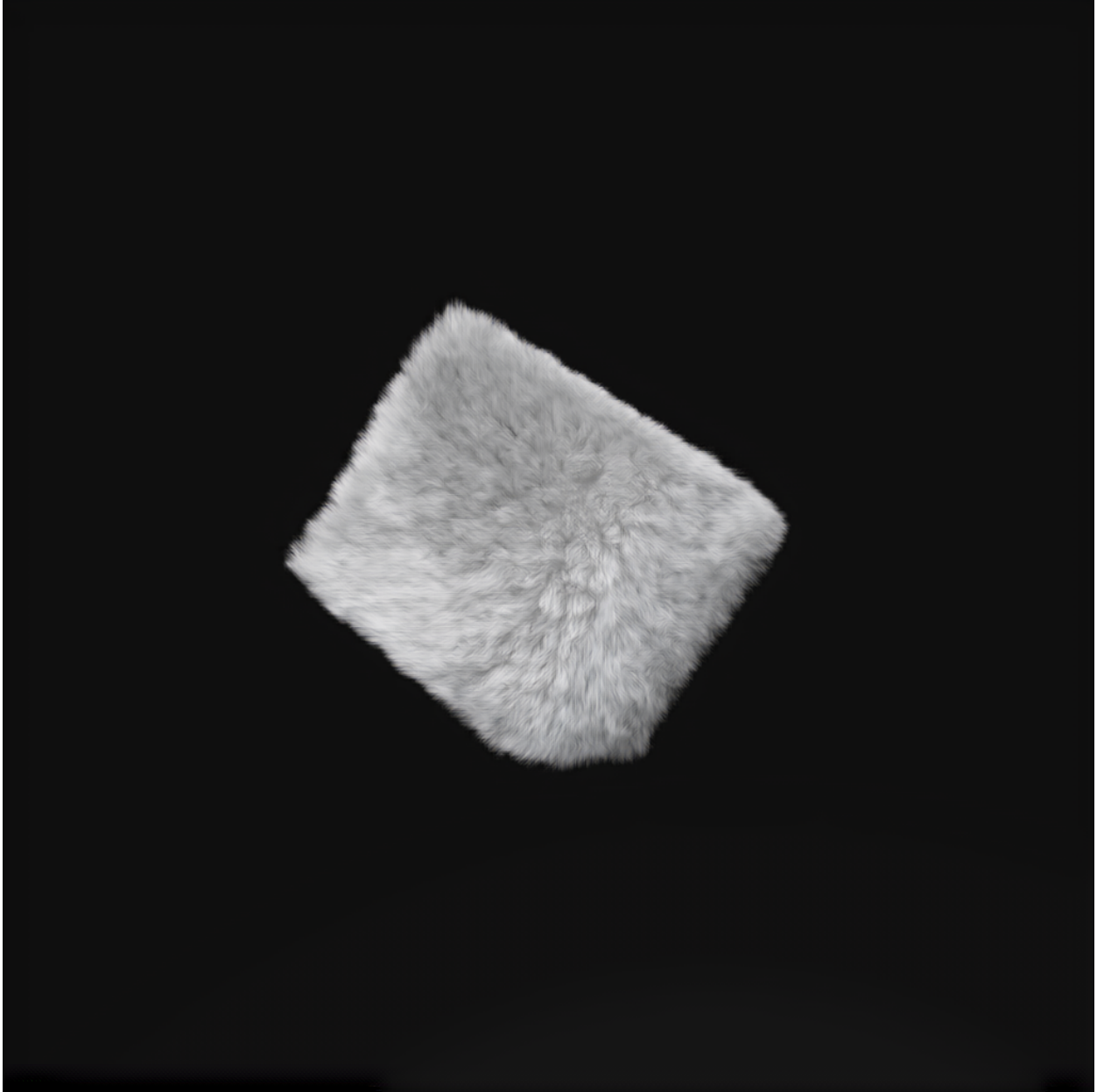


Figure 10: GAN-generated images when trained with SyntheticFur at high resolution.



Figure 11: GAN-generated images when trained with SyntheticFur at high resolution.



Figure 12: GAN-generated images when trained with SyntheticFur at high resolution.



Figure 13: GAN-generated images when trained with SyntheticFur at high resolution.



Figure 14: GAN-generated images when trained with SyntheticFur at high resolution.



Figure 15: GAN-generated images when trained with SyntheticFur at high resolution.